

Deep Ultraviolet Detector Based on Low-Temperature Fabricated ZnO/Ga₂O₃ Heterojunction

Guanhua Wu^{1,a}, Junlin Fang^{1,b}, Zhenhua Tang^{1,c,*}

¹School of Physics and Optoelectric Engineering, Guangdong University of Technology, Guangzhou Higher Education Mega Center, Guangzhou, 510006, China

^aguanhuawuh@163.com, ^bshuu3051@163.com, ^ctangzh@gdut.edu.cn

*Corresponding author

Abstract: The day-blind ultraviolet detector has been widely recognized due to its enormous potential in military and civilian applications such as missile tracking, flame detection, and electrical grid security. In comparison to the narrow bandgap semiconductor material Si, amorphous Ga₂O₃ is possessed of an ultra-wide bandgap, high-temperature resistance, high-pressure resistance, and the advantage of low-temperature and low-cost preparation, making it an ideal material for day-blind ultraviolet detectors. In this study, sol-gel and magnetron sputtering methods were employed to fabricate Ga₂O₃/ZnO heterojunction deep ultraviolet detectors. Compared to pure Ga₂O₃ detectors, a reduction in dark current by an order of magnitude was observed in the Ga₂O₃/ZnO heterojunction detectors. The photocurrent-to-dark current ratio increased by approximately 50 times, and the responsiveness increased by nearly an order of magnitude, resulting in a lower detection rate. This improvement can be attributed to the Ga₂O₃/ZnO heterojunction. Additionally, detector arrays were prepared, and the uniformity of the fabricated thin films was verified.

Keywords: Wide bandgap, deep ultraviolet detector, sol-gel method, amorphous gallium oxide, zinc oxide

1. Introduction

The day-blind ultraviolet detector operates in the day-blind wavelength range, where the light in this range is almost absent in the near-ground atmosphere, effectively isolating it from environmental interference. It plays a crucial role in military and civilian applications such as missile tracking, flame detection, electrical grid security, and environmental bio-detection [1-4]. To cope with harsh application environments, detectors need to withstand high temperatures, pressures, and radiation. Currently, Si-based deep ultraviolet detectors are a low-cost and mature solution. However, due to the small bandgap of Si, they require the use of filters, and Si's severe thermal instability inhibits high-temperature applications of the detectors [5]. Wide bandgap semiconductor materials, including AlGaN [6], MgZnO [4, 7], Ga₂O₃ [8], and diamond [9], are considered feasible alternatives to Si-based deep ultraviolet detectors. Ga₂O₃, in particular, with its ultra-wide bandgap (4.5-5.3 eV) directly corresponding to the day-blind wavelength range, high absorption coefficient for ultraviolet photons, structural stability at high temperatures and pressures, and low-cost preparation, is regarded as an ideal material for deep ultraviolet detectors [10-12].

Amorphous Ga₂O₃ has the advantages of low preparation temperature, no need to consider lattice mismatch issues, a wide range of substrate choices, and low difficulty in large-area film formation. It holds great potential in flexible devices and large-area image sensors [13]. However, issues such as high dark current, significant persistent photoconductivity effects, and low carrier mobility affect the optical detection capabilities (e.g., low detection rate, delayed response time, and responsiveness). Annealing is a viable solution that can improve the response speed of amorphous Ga₂O₃ but may result in a reduction in response current and deterioration of responsiveness [14]. To address this issue, researchers have composed Ga₂O₃ with other metal compounds to form heterojunction devices, achieving promising results [15-17]. Among them, ZnO, with its high electron mobility, low preparation temperature, and good response to the day-blind wavelength range, has shown good results in Ga₂O₃/ZnO heterojunction devices [18].

The study fabricated Ga₂O₃/ZnO heterojunction deep ultraviolet detectors, with Ga₂O₃ and ZnO prepared using the sol-gel method and magnetron sputtering method, respectively. For comparison, pure

Ga_2O_3 detectors were also prepared. Under 0V bias conditions, compared to pure Ga_2O_3 detectors, $\text{Ga}_2\text{O}_3/\text{ZnO}$ heterojunction detectors exhibited a reduction in dark current by an order of magnitude, a 50-fold increase in photocurrent-to-dark current ratio, nearly an order of magnitude increase in responsiveness, an 18.85 s decrease in response time, and a lower detection rate. These improvements can be attributed to the built-in electric field between Ga_2O_3 and ZnO heterojunction. Simultaneously, detector arrays were prepared to confirm the good uniformity of the thin films. The research results provide a feasible solution for deep ultraviolet detectors.

2. Experimental

The process begins by thoroughly mixing analytical-grade gallium nitrate, ethylene glycol, and ethanolamine, followed by stirring at 60°C for one hour. Subsequently, the mixture is left to stand at room temperature for 24 hours, resulting in a uniform and transparent Ga_2O_3 precursor solution with a concentration of 0.5 mol/L. Using n-Si as the substrate, the cleaning procedure involves sequentially placing the substrate in acetone, anhydrous ethanol, and ultrapure water for 10 minutes each, followed by drying with nitrogen gas.

Initially, ZnO thin film is sputtered on n-Si using magnetron sputtering. The sputtering chamber is evacuated to below 1×10^{-4} Pa using a combination of mechanical and molecular pumps. The substrate is then heated to maintain a stable temperature of 120°C, followed by the introduction of argon gas at a flow rate of 45 sccm. The pressure is maintained at 1.0 Pa, and the RF power is set to 100 W, with a sputtering time of 10 minutes.

Next, Ga_2O_3 is spin-coated onto the prepared ZnO film. The precursor solution is dropped onto the ZnO film, and spin-coating is performed at speeds of 1000 rpm and 3000 rpm for 10 seconds and 30 seconds, respectively. Subsequently, the coated substrate is heated at 100°C for 10 minutes and then at 300°C for 20 minutes, with this process repeated 15 times. Finally, the sample undergoes rapid thermal annealing at 400°C for one hour.

Ultimately, ion sputtering is employed to create gold electrodes on the Ga_2O_3 film, and indium electrodes are prepared on the n-Si substrate. As a control, Ga_2O_3 film is concurrently prepared on Si.

3. Results and Discussion

Figure 1(a) presents the XRD spectrum of $\text{Ga}_2\text{O}_3/\text{ZnO}$ heterojunction, with the XRD spectrum of Si substrate included for comparative analysis. From Figure 1(a), it can be observed that the diffraction peak at 34.4° corresponds to ZnO (PDF #76-1805), and peaks at 61.7°, 65.9°, and 69.4° correspond to Si (PDF#74-0534). No characteristic diffraction peaks related to Ga_2O_3 crystals are observed, indicating that the grown Ga_2O_3 film is amorphous. The thickness of Ga_2O_3 is measured to be 56 nm, and the thickness of zinc oxide is 52 nm using cross-sectional SEM. EDS testing on the cross-section confirms the presence of zinc oxide and gallium oxide, as demonstrated in the energy spectrum plot in Figure 1(c). Figures 1(d) to 1(f) display the distribution of elements in the cross-section.

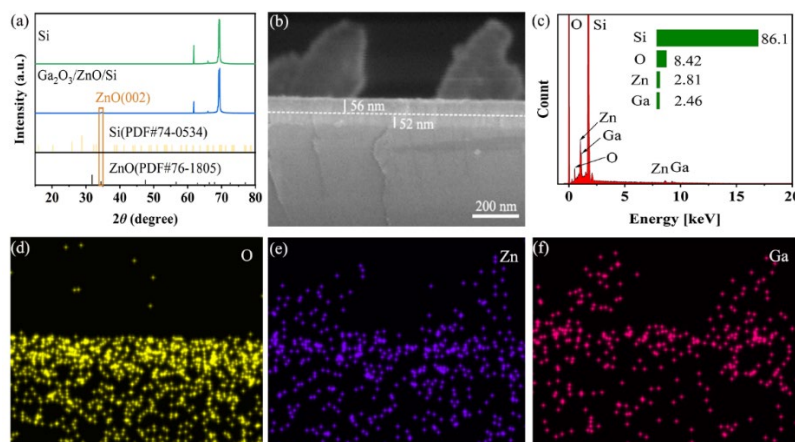


Figure 1: (a) XRD spectrum of $\text{Ga}_2\text{O}_3/\text{ZnO}$ heterojunction; (b) Cross-sectional SEM image of $\text{Ga}_2\text{O}_3/\text{ZnO}$ heterojunction; (c) EDS spectrum of $\text{Ga}_2\text{O}_3/\text{ZnO}$ heterojunction; (d) Elemental distribution of O; (e) Elemental distribution of Zn; (f) Elemental distribution of Ga

Figures 2(a) and 2(b) depict schematics of the Ga₂O₃/ZnO heterojunction and pure Ga₂O₃ detectors, respectively, where the contact between the electrode and crystal is a Schottky contact. In Figures 2(c) and 2(d), the IV curves of the Ga₂O₃/ZnO heterojunction detector and pure Ga₂O₃ detector are presented for both dark conditions and UV light exposure (254 nm, 5.76 μW/cm² for Ga₂O₃/ZnO/Si, and 254 nm, 9.95 μW/cm² for Ga₂O₃/Si). From the graphs, it is evident that at 0 V readout voltage, the current increases from 3.23×10⁻¹² A in the dark to 6.42×10⁻¹⁰ A under UV light exposure for Ga₂O₃/ZnO heterojunction detectors, resulting in a photocurrent-to-dark current ratio of approximately 199. Additionally, a short-circuit current of 6.42×10⁻¹¹ A and an open-circuit voltage of 0.13 V are observed, indicating that the detector can operate in photovoltaic mode. Figure 2(d) illustrates the IV curves for the pure Ga₂O₃ detector under dark conditions and UV light exposure (254 nm, 9.95 μW/cm²). At 0 V readout voltage, the current increases from 3.27×10⁻¹¹ A in the dark to 1.52×10⁻¹⁰ A under UV light exposure, resulting in a photocurrent-to-dark current ratio of approximately 5. The short-circuit current and open-circuit voltage are measured at 3.27×10⁻¹¹ A and 0.05 V, respectively.

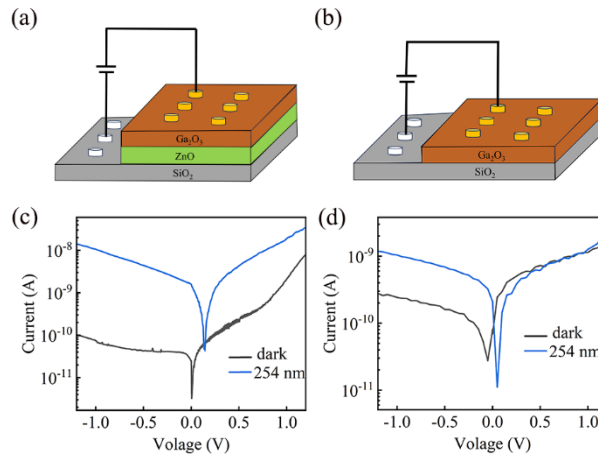


Figure 2: (a) Ga₂O₃/ZnO heterojunction detector schematic; (b) Pure Ga₂O₃ detector schematic; (c) IV curves of Ga₂O₃/ZnO heterojunction detector; (d) IV curves of Pure Ga₂O₃ detector.

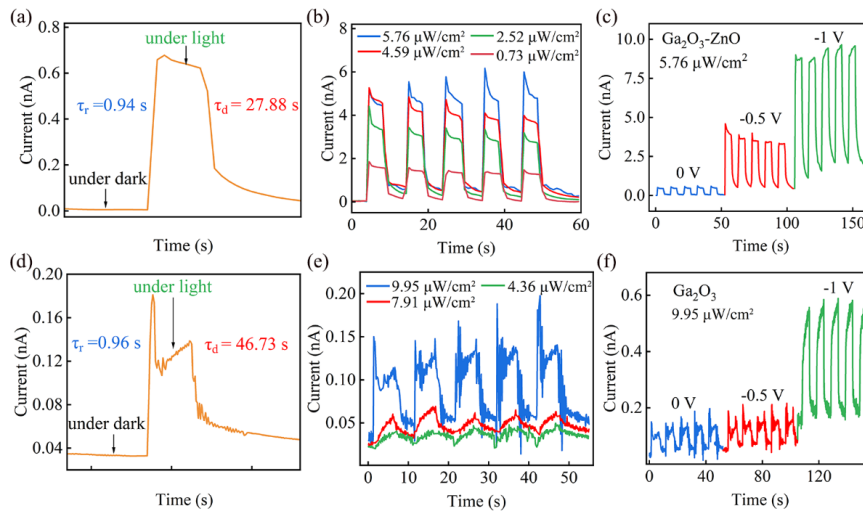


Figure 3: (a) Rise and fall times of the Ga₂O₃/ZnO heterojunction detector at 0 V bias; (b) Response curves of the Ga₂O₃/ZnO heterojunction detector under different light intensities; (c) Response curves of the Ga₂O₃/ZnO heterojunction detector at different biases; (d) Rise and fall times of the pure Ga₂O₃ detector at 0 V bias; (e) Response curves of the pure Ga₂O₃ detector under different light intensities; (f) Response curves of the pure Ga₂O₃ detector at different biases.

The response times of the Ga₂O₃/ZnO heterojunction and pure Ga₂O₃ detectors are shown in Figures 3(a) and 3(d). The rise time (tr, 10%-90% of saturated photocurrent) and fall time (td, 90%-10% of saturated photocurrent) for Ga₂O₃/ZnO heterojunction are approximately 0.94 s and 27.88 s, respectively, while for pure Ga₂O₃, tr and td are 0.96 s and 46.73 s. The light response curves over time, with varying light intensities applied to the devices, are illustrated in Figures 3(b) and 3(e). Under different light intensities, the photocurrent of the Ga₂O₃/ZnO heterojunction detector increases by approximately two

orders of magnitude, whereas the pure Ga₂O₃ detector increases by one order of magnitude under strong light. Both detectors maintain stability during continuous testing with five consecutive light pulses, indicating strong stability for Ga₂O₃/ZnO heterojunction and pure Ga₂O₃ detectors. From the graphs, it is observed that the devices exhibit an instantaneous peak state upon illumination. As shown in Figures 3(b) and 3(e), the photocurrent peaks immediately after illumination and then decreases to a stable state. This phenomenon is attributed to the accumulation of photo-induced charge carriers. Photo-induced charge carriers accumulate on the surface of Ga₂O₃ under UV light activation. These carriers cannot diffuse into ZnO and Si in a short time, resulting in a peak in the photocurrent. After the carriers diffuse through concentration gradients, the photocurrent gradually decays to a stable value. Maintaining a constant light intensity while changing the readout voltage, the light response curves of the devices are shown in Figures 3(c) and 3(f).

The light responsivity characterizes the efficiency with which a device generates electric current in response to incident light and is a crucial parameter for evaluating the device's performance and sensitivity. A high light responsivity typically indicates the device's ability to efficiently convert light energy into an electrical signal, demonstrating excellent optoelectronic performance. It can be calculated using the following formula^[19]:

$$R = \frac{I_{\text{photo}} - I_{\text{dark}}}{P \cdot S} \quad (1)$$

Where I_{photo} represents the photocurrent, I_{dark} is the dark current, P denotes the light intensity, and S represents the detector's area. According to the formula, the responsivity of Ga₂O₃/ZnO heterojunction and pure Ga₂O₃ detectors at 0 V can be calculated as 111 $\mu\text{A/W}$ and 12 $\mu\text{A/W}$, respectively, demonstrating an improvement of nearly an order of magnitude in responsivity. The normalized detectivity D^* is a key parameter used to quantitatively characterize the ability of a detector to detect weak signals. It can be calculated using the following formula^[20]:

$$D^* = \frac{R\sqrt{S}}{\sqrt{2qI_{\text{dark}}}} \quad (2)$$

Where R represents the responsivity, S represents the detector's area, and I_{dark} is the dark current. The normalized detectivity for Ga₂O₃/ZnO heterojunction is calculated to be 9.68×10^9 Jones (1 Jones = 1 $\text{cm Hz}^{1/2} \text{W}^{-1}$), while the normalized detectivity for pure Ga₂O₃ is 4.30×10^8 Jones.

To illustrate the photoelectric detection principle of the devices, energy band diagrams for both devices are provided. Figure 4(a) shows the energy band diagram before the contacts between different components. According to the literature, Ga₂O₃ has an electron affinity of 3.15 eV, a work function of 4.23 eV, and a bandgap of 4.95 eV. ZnO has an electron affinity of 4.5 eV, a work function of 4.65 eV, and a bandgap of 3.37 eV. For Si, these values are 4.05 eV, 4.25 eV, and 1.13 eV, respectively^[16, 21-23]. The energy band diagram for the pure Ga₂O₃ detectors is shown in Figure 4(b), where a Schottky barrier is formed between Au and Ga₂O₃, with a theoretical built-in potential of 0.87 eV. Another junction is formed between Si and Ga₂O₃, creating an internal electric field opposite to the Schottky direction. However, this barrier height is small (approximately 0.02 eV), insufficient to impede electron transport. Under illumination, photogenerated carriers in Ga₂O₃ are rapidly separated by the built-in electric field. The energy band diagram for the Ga₂O₃/ZnO heterojunction device is shown in Figure 4(c). A built-in electric field of 0.42 eV is formed at the ZnO-Ga₂O₃ interface, and another internal electric field of 0.4 eV is formed at the Si-ZnO interface. Both electric fields have the same direction, promoting the separation of electron-hole pairs and inducing faster carrier migration. Additionally, ZnO also responds to 254 nm light, enhancing the overall photoresponse of the device. Moreover, oxygen vacancies play a crucial role in the UV performance, and the Ga₂O₃/ZnO heterojunction contains more oxygen vacancies than pure Ga₂O₃, facilitating more effective transfer of photoexcited charge carriers. Therefore, the Ga₂O₃/ZnO heterojunction device exhibits a significant improvement in UV responsiveness compared to the pure Ga₂O₃ device.

To assess the uniformity of the prepared Ga₂O₃ film, a Ga₂O₃/ZnO heterojunction device array was fabricated on the same film. Under 0 V bias and illumination with an intensity of 5.76 $\mu\text{W/cm}^2$, the photoresponse of the detector array is depicted in Figure 4(d). It can be observed that the photocurrent shows minimal variation, with the maximum and minimum photocurrents being 0.494 nA and 0.478 nA, respectively, indicating a small deviation. Under 0 V bias, the photoresponse of the array under different light intensities is shown in Figure 4(e). As the light intensity increases, the photocurrent also increases, and there is minimal variation in the photoresponse among different devices. This suggests that the prepared Ga₂O₃ film exhibits uniformity.

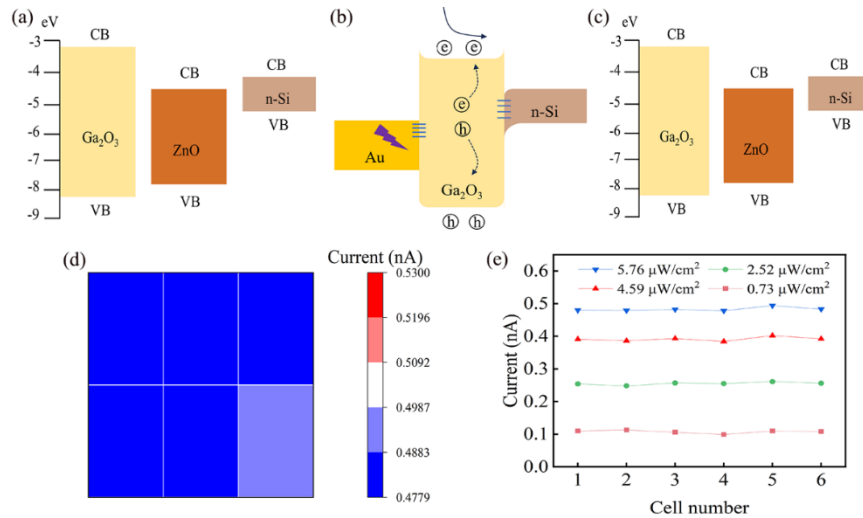


Figure 4: (a) illustrates the band diagram of the Ga₂O₃/ZnO heterojunction before contact; (b) depicts the band diagram of pure Ga₂O₃ under 254 nm light; (c) displays the band diagram of the Ga₂O₃/ZnO heterojunction under 254 nm light; (d) shows the photocurrent of the detector array under 0 V bias and illumination with an intensity of 5.76 μW/cm⁻²; (e) demonstrates the photocurrent response of the detector array under 0 V bias to incident light of varying intensities.

4. Summary

In this study, Ga₂O₃/ZnO heterojunction deep ultraviolet detectors were prepared using a sol-gel method and magnetron sputtering, in comparison to pure Ga₂O₃ detectors. The Ga₂O₃/ZnO heterojunction detector exhibited a one-order-of-magnitude improvement in dark current, photocurrent-to-dark current ratio, and responsivity compared to the pure Ga₂O₃ detector. The response time was reduced by 18.85 s, and a lower detection rate was achieved. The improvements were explained through band diagrams. Additionally, a detector array was fabricated, confirming the uniformity of the prepared films.

Acknowledgements

This work was financially supported by the National Natural Science Foundation of China (NSFC) (Grant No. 62073084, 51702055, 12172093, 11904056, and 11704079), Guangdong Provincial Natural Science Foundation of China (Grant No. 2023A1515011599), Guangzhou Basic and Applied Basic Research Foundation (Grant No. 202102021035), Open Foundation of Guangdong Provincial Key Laboratory of Electronic Functional Materials and Devices (Grant No. EFMD2021008M), Guangdong Provincial Overseas Master Program, Special Funds for the Cultivation of Guangdong College Students' Scientific and Technological Innovation (Climbing Program Special Funds, Grant No. pdjh2020a0174).

References

- [1] Bin Zhao, Fei Wang, Hongyu Chen, et al. An Ultrahigh Responsivity (9.7 mA W⁻¹) Self-Powered Solar-Blind Photodetector Based on Individual ZnO–Ga₂O₃ Heterostructures[J]. *Advanced Functional Materials*, 2017.
- [2] Razeghi M. Deep ultraviolet light-emitting diodes and photodetectors for UV communications [C]// *Optoelectronic Integrated Circuits VII*. SPIE, 2005, 5729: 30-40.
- [3] Zheng W, Zhang Z, Lin R, et al. High-Crystalline 2D Layered PbI₂ with Ultrasoft Surface: Liquid-Phase Synthesis and Application of High-Speed Photon Detection [J]. *Advanced Electronic Materials*, 2016, 2(11): 1600291
- [4] Hu Q, Zheng W, Lin R, et al. Oxides/graphene heterostructure for deep-ultraviolet photovoltaic photodetector[J]. *Carbon*, 2019, 147: 427-433.
- [5] Kang C H, Dursun I, Liu G, et al. High-speed colour-converting photodetector with all-inorganic CsPbBr₃ perovskite nanocrystals for ultraviolet light communication[J]. *Light: Science & Applications*, 2019, 8(1): 94.

- [6] Liu B, Chen D, Lu H, et al. Hybrid Light Emitters and UV Solar-Blind Avalanche Photodiodes based on III-Nitride Semiconductors[J]. *Advanced Materials*, 2020, 32(27): 1904354.
- [7] Chen H, Yu P, Zhang Z, et al. Ultrasensitive self-powered solar-blind deep-ultraviolet photodetector based on all-solid-state polyaniline/MgZnO bilayer[J]. *Small*, 2016, 12(42): 5809-5816.
- [8] Kong W Y, Wu G A, Wang K Y, et al. Graphene- β -Ga₂O₃ heterojunction for highly sensitive deep UV photodetector application[J]. *Adv. Mater.*, 2016, 28(48): 10725-10731.
- [9] Wei M, Yao K, Liu Y, et al. A solar-blind UV detector based on graphene-microcrystalline diamond heterojunctions [J]. *Small*, 2017, 13(34): 1701328.
- [10] Cui S, Mei Z, Zhang Y, et al. Room-temperature fabricated amorphous Ga₂O₃ high-response-speed solar-blind photodetector on rigid and flexible substrates[J]. *Advanced Optical Materials*, 2017, 5(19): 1700454.
- [11] Li Q, Lin J, Liu T Y, et al. Gas-mediated liquid metal printing toward large-scale 2D semiconductors and ultraviolet photodetector[J]. *npj 2D Materials and Applications*, 2021, 5(1): 36.
- [12] Kuramata A, Koshi K, Watanabe S, et al. High-quality β -Ga₂O₃ single crystals grown by edge-defined film-fed growth[J]. *Japanese Journal of Applied Physics*, 2016, 55(12): 1202A2.
- [13] Du S, Yu N, Lin X, et al. High performance ultraviolet A/ultraviolet C detector based on amorphous Ga₂O₃/ZnO Nanoarrays/GaN structure[J]. *Physica E: Low-dimensional Systems and Nanostructures*, 2022, 144: 115398.
- [14] Zhou C, Liu K, Chen X, et al. Performance improvement of amorphous Ga₂O₃ ultraviolet photodetector by annealing under oxygen atmosphere[J]. *Journal of Alloys and Compounds*, 2020, 840: 155585.
- [15] Wang H, Ma J, Cong L, et al. Solar-blind UV photodetector with low-dark current and high-gain based on ZnO/Au/ Ga₂O₃ sandwich structure[J]. *Materials Today Physics*, 2022, 24: 100673.
- [16] Li H, Li Y, Xiao G, et al. Simple fabrication ZnO/ β - Ga₂O₃ core/shell nanorod arrays and their photoresponse properties[J]. *Optical Materials Express*, 2018, 8(4): 794-803.
- [17] Jia M, Wang F, Tang L, et al. High-performance deep ultraviolet photodetector based on NiO/ β -Ga₂O₃ heterojunction[J]. *Nanoscale research letters*, 2020, 15(1): 47.
- [18] Bukke R N, Mude N N, Bae J, et al. Nano-scale Ga₂O₃ interface engineering for high-performance of ZnO-based thin-film transistors[J]. *ACS Applied Materials & Interfaces*, 2022, 14(36): 41508-41519.
- [19] Chen X, Ren F, Gu S, et al. Review of gallium-oxide-based solar-blind ultraviolet photodetectors[J]. *Photonics Research*, 2019, 7(4): 381-415.
- [20] Xu J, Zheng W, Huang F. Gallium oxide solar-blind ultraviolet photodetectors: A review[J]. *Journal of Materials Chemistry C*, 2019, 7(29): 8753-8770.
- [21] Quemener V, Alnes M, Vines L, et al. The work function of n-ZnO deduced from heterojunctions with Si prepared by ALD[J]. *Journal of Physics D: Applied Physics*, 2012, 45(31): 315101.
- [22] Liu Z, Liu Y, Wang X, et al. Energy-band alignments at ZnO/Ga₂O₃ and Ta₂O₅/Ga₂O₃ heterointerfaces by X-ray photoelectron spectroscopy and electron affinity rule[J]. *Journal of Applied Physics*, 2019, 126(4).
- [23] Li G, Zhang K, Wu Y, et al. Self-powered solar-blind ultraviolet photodetectors with Ga₂O₃ nanowires as the interlayer[J]. *Vacuum*, 2023: 112277.